guide partially loaded with ferrite," *Bell Syst. Tech. J.*, vol. 38, pp. 1427–1456, 1959.
e) W. L. Bongianni, "Magnetostatic propagation in a dielectric layered structure," *J. Appl. Phys.*, vol. 43, pp. 2541–2548, 1972.
f) D. F. Vaslow, "Group delay time for the surface wave on a YIG film backed by a grounded dielectric slab," *Proc. IEEE* (Lett.), vol. 61, pp. 142–143, Jan. 1973.
[10] a) L. K. Brundle and N. J. Freedman, "Magnetostatic surface waves on a Y. I. G. slab," *Electron. Lett.*, vol. 4, pp. 132–134, 1968.
b) R. Pauchard, B. Désormière, and J. Guidevaux, "Electromagnetic surface waves in a metallised ferrite slab," *Electron. Lett.*, vol. 7, pp. 428–430, 1971.
[11] a) B. Lax and K. J. Button, "Theory of new ferrite modes in rectangular wave guide," *J. Appl. Phys. Lett.*, vol. 26, pp. 1184–1185, 1955.
b) K. J. Button and B. Lax, "Theory of ferrites in rectangular waveguides," *IRE Trans. Antennas Propagat.*, vol. AP-4, pp. 531–537, July 1956.
[12] R. E. De Wames and T. Wolfram, "Characteristics of magnetostatic surface waves for a metalized ferrite slab," *J. Appl. Phys.*, vol. 41, pp. 5243–5246, 1970.

A New Interdigital Electrode Transducer Geometry

KENNETH M. LAKIN, MEMBER, IEEE, DAVID W. T. MIH, AND ROBERT M. TARR

***Abstract*—A new interdigital electrode transducer geometry has been conceived and its theoretical performance verified experimentally. The transducer is composed of sets of electrodes which are connected in series through an offset or "dog-leg" electrode, thereby significantly increasing the electrical impedance of the transducer over that of a conventional one having the same aperture. This transducer radiates and receives a uniform straight-crested wavefront. The transducer is shown to have unique impedance properties suited for wide-aperture surface-wave devices or those requiring some form of wave-amplitude weighting.**

Experiments have been conducted on *YZ* $LiNbO_3$ which verify that the terminal impedance of the transducer is proportional to the square of the number of equal-aperture constant-amplitude sections.

I. INTRODUCTION

INTERDIGITAL electrode transducers (IDT), employed for surface acoustic-wave generation, have a fundamental property that the terminal electrical impedance is inversely proportional to the width of the electrode overlap or beam aperture [1]. This property is exhibited if the electrode voltage is independent of aperture since then the displacement current is proportional to electrode area and, hence, width. A given transducer's width is chosen as a compromise between a number of factors which are: a) electrode conduction loss, b) capacitance and implied relative ease of tuning, c) resultant radiation resistance compared to source and load impedances which affects mismatch loss and surface-wave reflection (regeneration), d) diffraction effects due to propagation distance in relation to chosen width, and e) in some cases, available substrate size. Factor d) may be reduced by using wider apertures, which lower the electrical impedance, or diffraction loss may be compensated for by use of aperture weighting if the effects are accurately predictable. Narrow apertures may, however, be required in pulse-compression filter transducers [2] where a large array will have, at any one frequency, an active section in shunt with the large capacitance of the inactive region. The large shunt capacitance has the effect of transforming active section impedances to much lower values which can only be partially offset in magnitude by a small aperture design. Frequency or phase filter synthesis requires aperture weighting such that small electrode overlap regions have higher impedance and draw less current, hence radiate less power, than wider aperture regions. The classic rectangular passband frequency filter, for example, requires a sin x/x weighting in the transducer spatial domain where the spatial sidelobes of the sin x/x aperture distribution ultimately determine the frequency passband amplitude response. However, in a given fabrication, the spatial sidelobe overlap distribution may result in apertures of only a few wavelengths and, because of diffraction effects, the effective weighting of these spatial sidelobes is difficult to determine.

The point of the preceding discussion is to indicate the desirability of a transducer geometry which offers some flexibility in the relation between impedance and aperture. A desirable transducer might be composed of electrodes which radiate identical, or nearly identical, width waves yet having each electrode's efficiency determined by a parameter other than overlap aperture. This paper describes one approach, illustrated in Fig. 1, which employs interdigital electrode arrays arranged in a unique manner that results in a more flexible impedance versus aperture relationship, and radiates uniform plane waves from electrode pairs having the usual half-wavelength periodicity in the direction of propagation. A uniform straight-

Manuscript received December 6, 1973; revised April 8, 1974. This work was supported in part by the Air Force Office of Scientific Research under Contract AFOSR-72-2391, in part by the Joint Services Electronics Program through the Air Force Office of Scientific Research/AFSC under Contract F44620-71-C-0067, and in part by the Office of Naval Research under Contract N00014-67-0269-0018.

The authors are with the Electronic Sciences Laboratory, University of Southern California, Los Angeles, Calif. 90007.

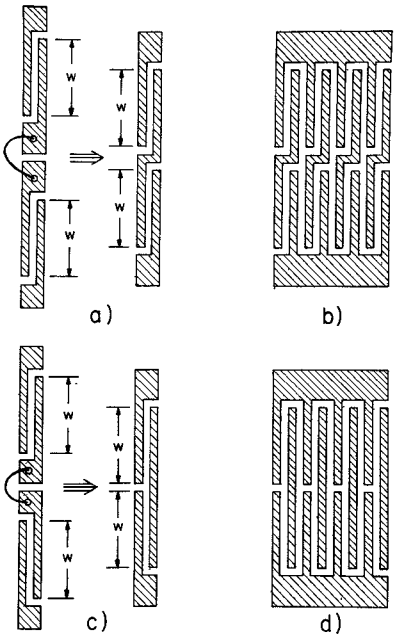

Fig. 1. Series electrode transducer configurations. (a) Evolution of two ordinary transducer elements into a uniform phase dog-leg element. (b) Array of dog-leg elements to form a four-electrode-pair transducer. (c) Evolution of two ordinary transducer elements into alternate phase elements. (d) Array of alternate phase elements to form a four-electrode-pair transducer.

crested wavefront is obtained by the jog crossover forming a "dog-leg" transducer (DLT). A geometry with series connection along the direction of propagation has been described previously by other authors [3], [4]. A parallel series combination of many finger pairs having narrow stripes in the direction of propagation has also been described [5].

Analysis of the electrical properties of the DLT has deliberately avoided reference to any particular transducer model and is based only upon an electrical equivalent circuit and the known fact that impedance must be inversely proportional to aperture in an IDT regardless of model. The impedance transforming properties of the transducer are derived and applied to the case of aperture weighting. Experimental results are reported which verify the important impedance transforming property.

II. THEORY

The dog-leg interdigital electrode transducer can be described electrically in terms of a series connection of conventional IDT's as shown in Fig. 1. The DLT evolves from the simple series connnection of IDT's as shown in Fig. 1(a) which then reduces to a jog or offset in one of the electrodes. The dog-leg electrode is offset one-half the fundamental wavelength in order to insure that the top and bottom halves of the transducer excite the same phase of surface wave for the same spatial location along the wavefront. A number of dog-leg sections may be combined into a multielectrode transducer in the usual manner suggested by Fig. 1(b).

Brief mention should be made of another possible series electrode transducer arrangement as indicated in Fig. 1(c). The construction follows as for the DLT, but results in a somewhat simpler electrode arrangement as shown in Fig. 1(d). Here the excited wave has opposite phases in top and bottom halves for equivalent spatial locations along the wavefront. The sudden phase change across the wavefront reduces the flexibility of this geometry for the traditional transducer applications because each section would tend to diffract independently as individual apertures in the far field. This geometry will not be considered further in this paper.

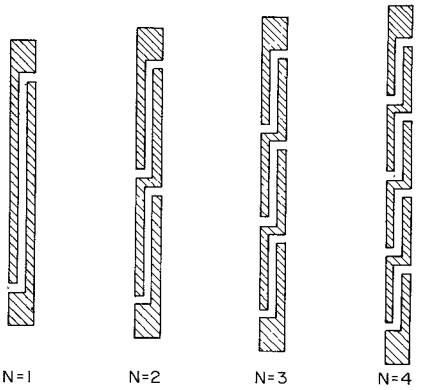

Fig. 2. Dog-leg transducers having various equal amplitude sections denoted by N.

The series connection for the DLT may be extended to higher order by the arrangement shown in Fig. 2. Only four cases are shown with N denoting the number of equal aperture sections with the case $N = 1$ being the normal IDT. In practice, the upper limit on N would be determined by the overall aperture and the requirement that at least a few wavelengths remain in each short aperture section. There would also be an increase in the conduction losses in the transverse segment, proportional to N, where the current is largest. However, as shown later, the maximum electrode current is reduced by N^{-2} and hence the resistive losses in these segments would be proportional to N^{-3}. The dog-leg or jog region will necessarily take up some space in the aperture and would introduce severe beam distortion unless the jog width is a small part of the section aperture. The crossover region could also be made diagonal although the rectangular geometry of Fig. 1 is more suited to photolithographic mask-making techniques.

Equivalent Circuits

Electrical-circuit characterization of the DLT can be developed without regard to any specific transducer model. This is possible by noting that transducer models differ in how equivalent-circuit parameters relate to material constants or the number of electrodes in the interdigital array. All transducer models can, in principle, arrive at either a series or parallel equivalent circuit represented by an impedance or admittance, respectively. The following properties exist for all transducer models. a) Simple network theory can be employed to transform between series and parallel equivalent circuits of any one

model. b) All transducer models must predict the same variation in impedance or admittance, with change in apertures for apertures larger than a few wavelengths. (For constant electrode voltage the complex displacement current is proportional to the aperture width.) c) For the IDT, the geometric capacitance is independent of frequency and proportional to the absolute aperture width. Fig. 3(a) shows the series equivalent circuit and Fig. 3(b) the parallel equivalent circuit where we note

$$R_a = \frac{G_a}{G_a^2 + (B_{c'} + B_a)^2} \quad \text{series radiation resistance} \tag{1a}$$

$$X_a = \frac{-B_a}{G_a^2 + (B_{c'} + B_a)^2} \quad \text{series acoustic reactance} \tag{1b}$$

$$X_c = \frac{B_{c'}}{G_a^2 + (B_{c'} + B_a)^2} \quad \text{series capacitive reactance} \tag{1c}$$

G_a = parallel radiation admittance (1d)

B_a = parallel acoustic susceptance (1e)

$B_{c'}$ = parallel capacitive susceptance. (1f)

In the absence of an acoustic interaction, the series and parallel capacitances are equal to the geometric capacitance. Also note that if B_a is equal to zero then so is X_a. Accordingly, we will define a quantity

$$Q_r \triangleq \frac{X_c}{R_a}\bigg|_{X_a=0} = \frac{B_{c'}}{G_a}\bigg|_{B_a=0} \tag{2}$$

and for the purposes of this paper refer to Q_r as the radiation Q. The condition when $B_a = 0$, or equivalently, $X_a = 0$, will be called synchronism and the associated frequency, the synchronous frequency.

The transducer impedance Z is inversely proportional to the width of the transducer aperture and may be described by

$$Z = z/w \tag{3a}$$

where

w = aperture width

z = impedance·length product (ohm·centimeter)

or

$$z = \rho_a + j(x_c + x_a) \tag{3b}$$

where

ρ_a = radiation resistance·length product (ohm·centimeter)

x_c = series capacitive reactance length product (ohm·centimeter)

x_a = series acoustic reactance length product (ohm·centimeter).

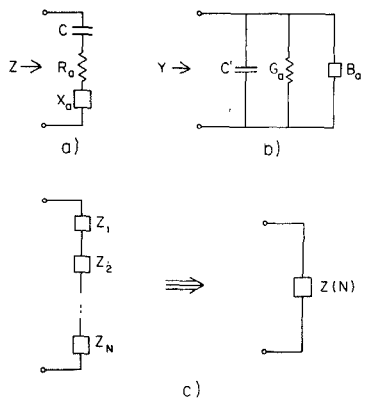

Fig. 3. Equivalent circuits for transducer sections. (a) Series equivalent with geometric capacitance C, radiation resistance R_a, and radiation reactance X_a. (b) Parallel equivalent circuit with capacitance C', radiation conductance G_a, and susceptance B_a. (c) Series representation of N elements having equivalent circuit of (a) and their combined impedance $Z(N)$.

A similar equation may be written for the admittance:

$$Y = yw$$

where

y = admittance per unit length (mho/centimeter).

Equations (3a) and (3b) constitute a convenient normalization of (1a)–(1c) with the aperture width introduced as a variable. In practice the normalized impedances are often expressed in units of ohm·wavelength rather than ohm·centimeter, and hence w is given in units of λ_0, the fundamental periodicity of the interdigital array. From the previous equations it is apparent that Q_r is independent of the aperture. Also note that the equations do not refer to any specific number of electrode pairs since only the aperture dependence is of interest and not the absolute values of the quantities.

DLT Analysis

The input impedance of the DLT is most easily obtained by considering a series connection of N IDT's as illustrated in Fig. 3(c). Thus each section of the DLT is assumed to have the impedance, given by (3a), of an IDT having identical aperture. The DLT impedance is

$$Z(N) = \sum_{i=1}^{N} Z_i \tag{4a}$$

where

$Z_i = z/w_i$ = impedance of the ith section from (3a)

where

w_i = aperture of the ith section.

If the apertures are all equal, then

$$Z(N) = NZ_s \tag{4b}$$

where

Z_s = impedance of each equal section.

It is useful to compare $Z(N)$ to the impedance of an IDT with the same total equivalent aperture. Thus, from (3a), the impedance of the IDT with total aperture

Nw is

$$Z(1) = Z_s/N \tag{5}$$

and finally from (4b) and (5)

$$Z(N) = N^2 Z(1). \tag{6}$$

The DLT with N equal sections has N^2 times the impedance of an IDT with equivalent aperture and radiates a wavefront which is essentially identical to the IDT. The disturbance in radiation near the electrode jog will be insignificant when the regions are small compared to the overall section aperture. The radiation Q for the DLT is given by

$$Q_r(N) = \frac{X_c(N)}{R_a(N)} = \frac{X_c}{R_a} = Q_r$$

and is found to be independent of the number of aperture sections N. Thus, for the same number of electrode pairs and transducer impedance, a DLT would exhibit identical frequency response as an IDT ($N = 1$) and thus have the same bandwidth. The radiated beamwidth would be larger by the factor N^2.

Conduction Losses

Of importance to the design of high-frequency and/or wide-aperture transducer arrays is the conduction loss in the electrode metallization [6]. The estimated sheet resistance for 500-Å aluminum films, as employed in UHF transducers or transducers fabricated by the lift-off technique is approximately 0.6 Ω/square. The net series ohmic resistance may then be expressed in general by

$$R_e = \tfrac{8}{3}\rho_s w_0$$

where

ρ_s = sheet resistance (ohms/square)

w_0 = aperture in interdigital periods λ_0.

The factor of 8/3 comes from a number of assumptions which are: a) that the current decreases linearly along an electrode, giving a factor of 1/3, b) that adjacent electrodes are in series with respect to conduction current, giving rise to a factor of 2, and finally, c) a factor of 4 if the electrode width is effectively one-fourth the fundamental electrode periodicity λ_0.

The radiation resistance as a function of aperture may be expressed as

$$R_a = \rho_a/w_0$$

where

ρ_a = radiation resistance in ohm period, $\Omega \cdot \lambda_0$.

Note in particular that R_a decreases with aperture whereas R_e increases with aperture. The aperture where $R_a = R_e$ is given by

$$w_{0c} = \left(\frac{3\rho_a}{8\rho_s}\right)^{1/2} \quad \text{in } \lambda_0.$$

Examples:

a) *ST* Quartz, 500-Å Al

$$\rho_a = 1.8 \times 10^3\ \Omega \cdot \lambda_0$$

$$\rho_s = 0.6\ \Omega/\text{square}$$

$$w_{0c} \simeq 34\ \lambda_0$$

b) *YZ* $LiNbO_3$, 500-Å Al

$$\rho_a = 7.340 \times 10^3\ \Omega \cdot \lambda_0$$

$$\rho_s = 0.6\ \Omega/\text{square}$$

$$w_{0c} = 68\ \lambda_0.$$

Values of ρ_a are taken from [6] as calculated by the procedure in [1]. If the aperture is smaller than w_{0c}, then most of the input electrical power is dissipated in the form of acoustic radiation, whereas if $w_0 > w_{0c}$, more conduction loss than radiation would occur.

For the DLT, R_e is essentially the same as for an IDT of identical aperture and number of electrode pairs since it results from a series addition in each case. However, the DLT radiation resistance becomes

$$R_a(N) = N^2\rho_a/w_0$$

and w_{0c} is, accordingly,

$$w_{0c}(N) = N\left(\frac{3\rho_a}{8\rho_s}\right)^{1/2}.$$

Thus the DLT aperture may be increased by a factor of N over the IDT while maintaining the same ratio of conduction loss to acoustic radiation. Alternatively, the DLT sheet resistance could be larger by N^2 and still maintain the same ratio of conduction loss to radiation loss for the same aperture.

The transverse segment resistance would increase proportionally to N yet the power dissipation would be proportional to N^{-3} as mentioned previously. Only when the number of wavelengths in an aperture section is small, near one or two, would this additional loss be appreciable.

Aperture Weighting

In filter design it is often necessary to change the transducer aperture as a function of distance along the propagation direction [7]. The acoustic beam weighting for an IDT is accomplished by changing the aperture as shown in Fig. 4(a) and (b) giving rise to a change in the electrical impedance according to (4a). Since all electrodes are in parallel, the individual electrode currents and radiated power are in direct proportion to the aperture width if the conduction loss is not too large [6]. The IDT weighted according to Fig. 4(b) exhibits an impedance given by

$$Z^{\text{IDT}}(\nu) = Z^{\text{IDT}}(0)\left(\frac{1}{1-\nu}\right) = Z^{\text{IDT}}(0)\left(1 + \frac{\nu}{1-\nu}\right) \tag{7}$$

where

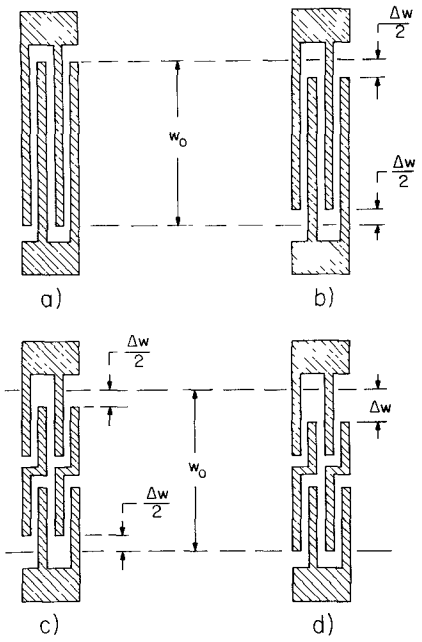

Fig. 4. Transducer aperture weighting configurations. (a) Normal IDT unweighted with aperture w_0. (b) Normal IDT with symmetrical weighting. (c) $N = 2$ DLT with symmetrical weighting but applicable to N sections. (d) DLT with unsymmetrical weighting.

$$\nu = \frac{\Delta w}{w_0}$$

w_0 = unweighted aperture

Δw = aperture weighting.

A DLT has an inherent weighting in that the impedance is proportional to N^2 for fixed aperture and thus gives rise to an effective weighting of the radiated energy. However, the quadratic dependence may not be convenient for a given design implementation and some form of aperture weighting may be desirable. Such an aperture weighting can take two forms, both of which depart from the desirable constant-width aperture. The first technique would be to uniformly decrease the width of each aperture section [Fig. 4(c)] of the DLT and produce a radiated power in a linear manner implied by (7). The overall aperture decrease need not be too severe since a different N value may be chosen in order to keep nearly the same beamwidth at reduced radiated power. For example, an $N = 5$ DLT uniformly aperture weighted by the factor 0.69 radiates the same power as an unweighted $N = 6$ DLT (or an $N = 1$ IDT weighted by a factor of 0.028). Thus the utility of the DLT is to maintain a more nearly uniform aperture width yet allow a considerable reduction in the radiated power. A second method of DLT weighting would be to decrease the aperture of one end section only such as in Fig. 4(d) giving rise to an impedance

$$Z^{\mathrm{DLT}}(N,\nu) = Z^{\mathrm{DLT}}(N,0)\left[1 + \frac{\nu}{1 - N\nu}\right], \qquad N = 1,2,\cdots.$$

The radiated power is proportional to the reciprocal of this impedance even though the wave amplitude is now nonuniformly distributed across the active aperture. The nonuniform amplitude across the beam front now would complicate the diffraction characteristics and effective weighting as determined by integration over the receiving transducer aperture. However, end weighting alone would be useful, if Δw were kept small compared to w_0/N, in order to obtain only a slight trimming without having to alter each aperture section.

III. EXPERIMENT

A series of experiments were performed in order to verify the major theoretical predictions of the DLT given by (6). Ten-electrode-pair transducers of $N = 1$ IDT and $N = 2$ DLT were fabricated on YZ $LiNbO_3$ using Al metallization. The transducers had a 101.6-μm fundamental wavelength, quarter-wavelength-wide electrodes and gaps, and a 5.08-mm aperture (50 wavelengths). The transducers' capacitances were 5.2 pF for the $N = 2$ transducer and 21.0 pF for the $N = 1$ transducer as measured at 10 kHz on a three-terminal capacitance bridge.

Radiation resistance was calculated from reflection coefficient measurements performed on a Hewlett-Packard 8407A network analyzer. The transducer impedance characteristics shown in Fig. 5 were measured under conditions of acoustic isolation. The actual impedances were calculated as a function of frequency from the magnitude and phase measurements of the reflection coefficient because of the increased precision. Background conduction loss associated with electrode metallization and tuning coil was determined by measurements made at the first null below center frequency where the surface-wave radiation resistance is zero as implied by transmission measurements. From the electrical parameters (Table I) it can be shown that the ratio of capacitance is 4.03:1, and the ratio of radiation resistance values is 4.04:1. This slight discrepancy is due to the fact that the effective aperture of the $N = 2$ transducer is approximately one-half wavelength less than the $N = 1$ transducer because of the dog-leg crossover region.

Transmission measurements between an $N = 1$ and $N = 2$ transducer are shown in Fig. 6. The response is essentially identical to the transmission between two normal transducers where the absence of a sharp null in the high-frequency sidelobes is due to bulk radiation, as determined by measuring transmission with absorber between transducers, and is characteristic of YZ $LiNbO_3$ with ten-electrode-pair transducers [8]. The surface-wave transmission path length was 1.016 cm with the underside of the substrate roughened in order to scatter most of the bulk waves. The calculated insertion loss due to impedance mismatch and residual conduction loss was 8.4 dB, and with a 6-dB assumed bidirectional loss the

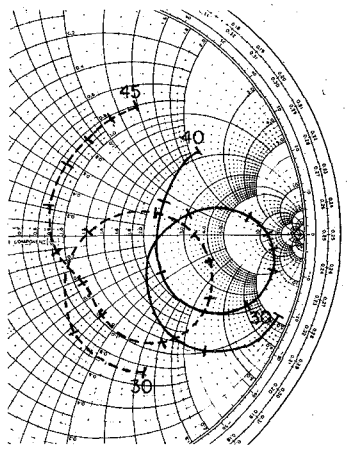

Fig. 5. Experimental results, Smith chart display of the $N = 1$, dashed, and $N = 2$ transducers tuned to near resonance. Tick marks represent 1-MHz frequency intervals.

TABLE I
MEASURED ELECTRICAL PARAMETERS OF TRANSDUCERS

Transducer	Capacitance pF	Loss Resistance ohms	Peak Resistance ohms	Radiation Resistance ohms
N = 1	21.0	35.1	177.9	-142.8
N = 2	5.2	32.6	609.7	577.1

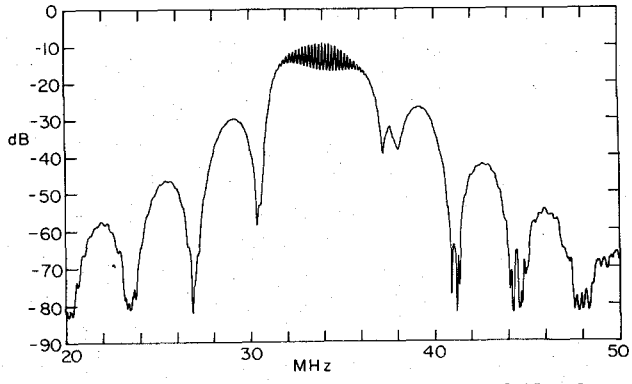

Fig. 6. Measured transmission between $N = 1$ and $N = 2$ transducers separated by 1.5 cm. The mid passband ripple is due to triple transit.

total insertion loss would be 14.4 dB. By averaging the triple transit ripple of Fig. 6, an insertion loss of 14 dB is obtained in close agreement with the predicted value. The multiple transit ripple of approximately 9 dB is consistent with the very high ratio of DLT radiation resistance (577 Ω) to load resistance (50 Ω). Since both ransducers were tuned at center frequency but not conjugately matched, the high ratio of radiation resistances to 50 Ω causes a large acoustic reflection coefficient and hence the 9-dB ripple. The ripple then is not an inherent property of the DLT itself but rather a phenomenon associated with the extreme mismatch condition. Based upon the impedance values (Table I) the calculated multiple ripple is approximately 10 dB for a calculated acoustic reflection coefficient of 0.87 and 0.63 of the $N = 2$ and $N = 1$ transducers, respectively.

IV. SUMMARY

A new interdigital electrode transducer geometry has been conceived and its theoretical performance verified experimentally. The transducer is composed of sets of series-connected electrodes which radiate a uniform phase front. If the transducer is composed of N equal-aperture-width sections, then the wave-amplitude distribution is also uniform across the wavefront and exhibits a terminal impedance which is N^2 times that of a normal transducer having the same effective aperture width.

Experimental measurements have been conducted on $N = 1$ and $N = 2$ transducers in order to verify the fundamental impedance transforming property. Results show that the impedance transforms as predicted and that the dog-leg crossover region does not introduce measurable spurious responses.

The new transducer is thought to be most usefully employed in tapped delay lines, pulse-compression filters, and frequency filters where wide apertures and aperture weighting are employed.

REFERENCES

[1] W. R. Smith, H. M. Gerard, J. H. Collins, T. M. Reeder, and H. J. Shaw, "Design of surface wave delay lines with interdigital transducers," *IEEE Trans. Microwave Theory Tech. (Special Issue on Microwave Acoustics)*, vol. MTT-17, pp. 865–873, Nov. 1969.

[2] H. M. Gerard, W. R. Smith, W. R. Jones, and J. B. Harrington, "The design and applications of highly dispersive acoustic surface-wave filters," *IEEE Trans. Microwave Theory Tech. (Special Issue on Microwave Acoustic Signal Processing)*, vol. MTT-21, pp. 176–186, Apr. 1973.

[3] A. J. Bahr, R. E. Lee, and A. F. Podell, "The grating array: A new surface acoustic wave transducer," *Proc. IEEE* (Lett.), vol. 60, pp. 443–444, Apr. 1972.

[4] A. J. De Vries, R. L. Miller, and T. J. Wojcik, "Reflection of a surface wave from three types of ID transducers," in *1972 IEEE Ultrasonics Symp. Proc.* (Boston, Mass., Oct. 4–7, 1972), pp. 353–358.

[5] D. T. Bell, Jr., and D. W. Mellon, "Development of an L-band pulse compressor using surface waves " in *IEEE Int. Microwave Symp. Digest* (Univ. Colorado, Boulder, June 4–6, 1973), pp. 126–128.

[6] K. M. Lakin, "Electrode resistance effects in interdigital transducers," *IEEE Trans. Microwave Theory Tech.*, to be published.

[7] R. H. Tancrell and M. G. Holland, "Acoustic surface wave filters," *Proc. IEEE*, vol. 59, pp. 393–409, Mar. 1971.

[8] M. R. Daniel *et al.*, "Acoustic radiation by interdigital grids on $LiNbO_3$," *J. Appl. Phys.*, vol. 43, pp. 4872–4875, Dec. 1972.